

DEVELOPMENT OF AN MCNP-BASED CALCULATIONAL MODEL FOR SEGMENTED TYPE SELF-POWERED NEUTRON DETECTORS

S. Fehér, J. Kópházi, G. Pór, Sz. Czifrus

Institute of Nuclear Techniques
Budapest University of Technology and Economics
Műegyetem rkp. 9, H-1111 Budapest, Hungary
fehers@reak.bme.hu

P.F.A. de Leege

Interfaculty Reactor Institute
Delft University of Technology
Mekelweg 15, NL-2629 JB Delft, The Netherlands
leege@iri.tudelft.nl

ABSTRACT

Recently a new idea has been proposed on constructing Self Powered Neutron Detectors (SPNDs) of more complex geometry, which could provide information not only on the local neutron flux, but also about its gradient. Such detectors could be used for neutron current measurements, which makes it possible to localize the vibrations in the reactor core. The development of these segmented type SPNDs requires the application of a modelling tool that is capable of calculating in complex geometries the coupled neutron, gamma and electron transport processes taking place in SPNDs. This paper outlines the first part of the investigation, the main objective of which is to elaborate an MCNP based computational model and code system satisfying the above requirements. Since no benchmark-type measurement data have been found in the literature, the authors performed a reference measurement that made it possible to separately study the electron transport processes from the neutron and background gamma photon reactions. The measurement was performed on a conventional cylindrical geometry SPND with rhodium emitter. During the evaluation of the measurement a current component of unknown origin was revealed. This component may have significant influence on the interpretation of the detector signal occurring in transient conditions. Modelling of the measurement using the code MCNP, supplemented with a self-developed program for the calculation of the electrostatic field, have proven to be suitable for the detailed tracking of the simultaneous neutron-photon-electron transport processes. However, due to the discrepancy between the calculated and measured detector current, furthermore the uncertainty of some nuclear data and parameters (cross sections, half-lives, beta spectrum etc.) the authors believe that it would be useful to initiate a calculational SPND intercomparison project on a well-established benchmark measurement.

1. INTRODUCTION

Recently a new idea has been proposed on constructing Self Powered Neutron Detectors (SPNDs) of more complex geometry (e.g. containing more than one emitter, or an emitter of non-cylindrical shape), which could provide information not only on the local neutron flux, but also about its gradient. Such detectors could be used for neutron current measurement, making it possible to localize the vibrations in the reactor core [1-3]. The development of this type of detectors requires a proper

computational modelling tool. In view of the complex geometry, the transport of neutrons, photons and electrons can effectively and precisely be studied only using appropriate Monte Carlo simulations.

The main objective of the research, part of which is outlined in the paper, is to develop a reliable computational model and code system, which make possible the investigation of the processes taking place in SPNDs in various detector geometries.

As a base for the calculational model suitable for the segmented types of SPNDs the code MCNP was selected, since it is capable of simulating the coupled neutron-gamma-electron transport processes of SPNDs in practically any complex geometries. A further consideration is that the 4C version of MCNP [4] has major improvements in electron transport algorithms. However, the MCNP itself is not able to calculate the effect of the electric field caused by the space charge of low energy beta particles „stopped” in the insulator. Thus, our computational model has been completed with an own developed program (INSPOT) suitable for electric field calculation.

On the other hand, the development of a code system capable of modelling SPNDs should obviously rely on measurement-based validation data. However, neither such data nor any corresponding benchmark measurements have been found in the literature. Therefore, we decided to perform an easy to model reference measurement, which provides the opportunity to separately study the electron transport processes from the neutron and background gamma photon reactions. During the reference measurement the delayed signal of a rhodium emitter SPND of simple cylindrical geometry was measured, separately from the other signal components.

In the present paper this reference experiment, along with the evaluation, is described, and a comparison with the Monte Carlo calculational results together with a sensitivity analysis is given.

2. REFERENCE MEASUREMENT

2.1. PRINCIPLE AND CONDITIONS OF THE MEASUREMENT

The reference measurement was performed in the research reactor of the Budapest University of Technology and Economics. The detector was placed in a cylindrical holder made of aluminum. Polyethylene spacers ensured that the detector was in the centerline of the holder. The irradiation location was selected such that it was far from any core irregularities and gradient of the flux was low. The principle of the measurement procedure is shown in Fig. 1.1. At the beginning, the detector (along with the holder) was inserted between the fuel rods.

Afterwards the reactor was started. Small power changes were made in order to test whether the detector signal follows these changes as theoretically expected, i.e. at a time lag characteristic to rhodium. This was followed by a longer (50 minutes) steady state operation at 100 kW. The detector current stabilized as the rhodium reached saturation activity. At this point the reactor was quickly shut down and a few seconds later the detector was removed from the core and lifted to a height of 1 m above the core, where it was fixed. At this location the neutron and gamma radiation from the core was negligible, thus the detector current, which was recorded using a computerized data acquisition system, could only be originating from the decay of the activated rhodium nuclei (and possibly other activation products). When the detector was being removed, very small however well observable stiction current fluctuations were measured for a period of less than 10 seconds. During the evaluation this starting transient period was not taken into account.

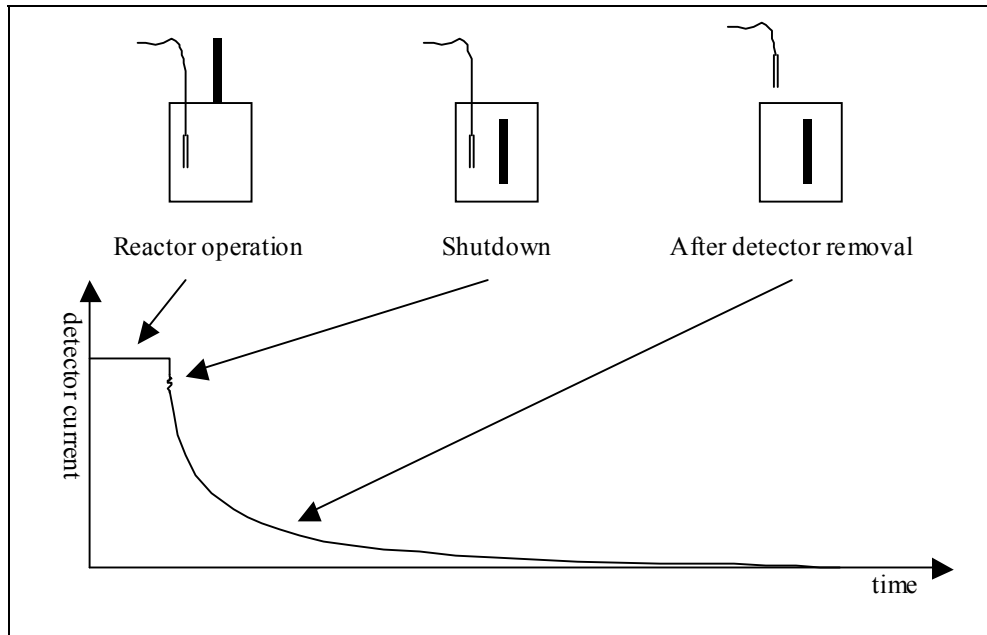


Figure 1. Scheme of the performance of the measurement

2.1. EVALUATION OF THE DETECTOR SIGNAL VS. TIME FUNCTION

The main objective of the analysis of the measured detector signal was the precise determination of the equilibrium (during reactor operation) value of the current component corresponding to the decay of rhodium. On the other hand, the thorough investigations revealed the fact that the current consists not only of this component but also some other component is present.

The time behaviour of the current reflected the two exponential components expected from the decay scheme of ^{104}Rh (see Fig 2.). Based on this observation, first a function of the form

$$I(t) = Ae^{-\lambda_g t} + Be^{-\lambda_m t} + C \quad (1)$$

was fitted on the curve. The decay constants of the ground and metastable states (λ_g and λ_m , respectively) were assumed known, while the initial (saturation) activities (A és B) and the value of the possibly present constant background (offset) was searched for. Although the assumption that the current changes only according to the decay of rhodium implies that A/B is constant, this ratio was observed to change as the time interval used for the fitting shifted away from the time of shutdown. Consequently, the detector signal contains a constituent different from the original assumption. For a more detailed analysis, A/B was chosen constant, while the fitting was performed using a function of the form

$$I(t) = De^{-E \cdot t} + Ae^{-\lambda_g t} + Be^{-\lambda_m t} + C \quad (2)$$

The best fit yielded a component with an initial weight of $7 \pm 1,6\%$ and effective half-life of 24 ± 6 s. The large magnitude of the uncertainties are mainly due to the comparatively large (approx. 1%) uncertainty of the half-life of ^{104}Rh [6]. After subtracting the component of unknown origin, the value of the saturation current is 18.0 ± 0.7 nA.

The above described component of unknown origin may particularly be important since it is most probably present in the equilibrium signal of the detector, thus having significant influence on the detector response to transients. One may rightly pose the question whether other detectors with rhodium emitter widely applied in NPPs also have the same component.

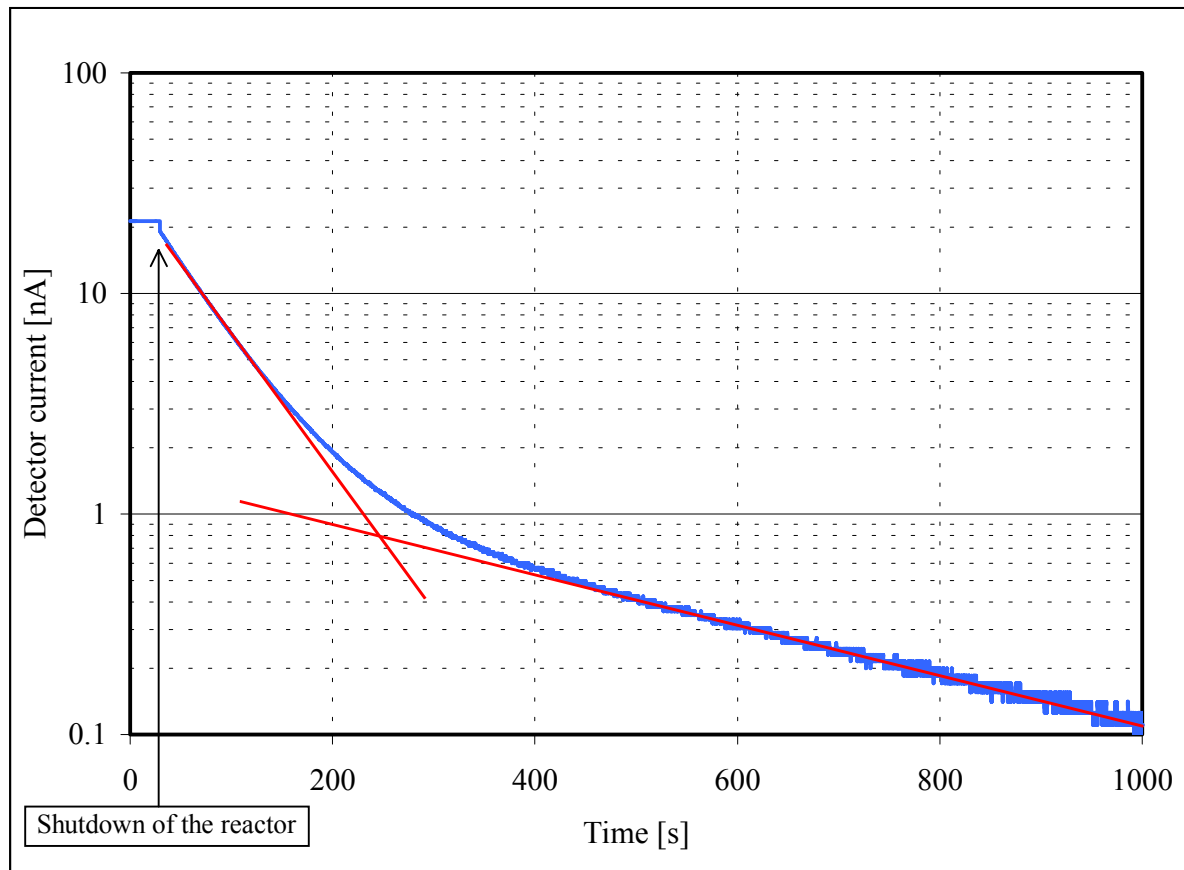


Figure 2. The detector current vs. time during the reference measurement

Concerning the origin of the above described component, the detection of which was made possible by the special „sterile” circumstances of the reference measurement, presently we only have suspicions. It might be (however not very probable) that the activation of some material present in the detector (e.g. impurity in the emitter) is responsible. One potential cause that naturally came up was the activation of the aluminum (99.5% purity) detector holder, but the calculations have shown that the beta decay with the accompanying gamma photons may only give rise to a signal contribution several orders of magnitude smaller. Furthermore, the half-life of the activation product (more than 2 minutes) is far longer than the time constant of the studied component. With the aid of thorough calculations two other potential causes could be excluded: the remaining gamma radiation of the core and the energetic gamma decay of the ^{16}N produced from oxygen in (n,p) reactions both in the water and in the insulator. Another assumption is that the component in question is due to the decay of ^{106}Rh , which is produced in two consecutive neutron captures from $^{104\text{m}}\text{Rh}$. This idea seems to be substantiated by the half-life of ^{106}Rh (29 s) and the very large capture cross sections of both $^{104\text{m}}\text{Rh}$ and ^{105}Rh . However, in order to prove this explanation further calculations will have to be performed. On the other hand, it might also be possible that some non-nuclear phenomenon (e.g. electrostatic) is responsible for this effect.

3. MODELLING OF THE REFERENCE MEASUREMENT USING MCNP

In this section those calculations are described which were used in order to compute the saturation current of the detector with the aid of MCNP. Since this code is not capable of modelling the electrostatic field evolving in the insulator, the electrostatic effects were accounted for through the application of the program INSPOT developed by the authors.

3.1. STEPS OF MODELLING

The modelling of the reference measurement was done in two parts. First the neutron flux distribution and the reaction rate of the neutron capture reactions were determined for different regions of the emitter while the detector was placed into the reactor. In this step a neutron-only calculation (*mode n*) was performed on the reactor model (containing the detector of course).

After determining the value and spatial distribution of the reaction rate of neutron capture inside the emitter, assuming a stationer irradiation (equilibrium state) this distribution was taken equivalent to that of the electrons emitted from beta decays. Accordingly, in the second step of modelling this source distribution was applied for the detailed transport calculation of photons and electrons. The second step was obviously carried out using a simpler MCNP model containing the detector and immediate vicinity only.

3.2. GEOMETRY AND MATERIAL COMPOSITION OF THE DETECTOR

Our information on the SPND used for the reference measurement was mainly based on [5]. The cross sectional view of the detector from that publication is shown in Fig 3. The dimensions and materials are summarized in Table I (also based on [5]).

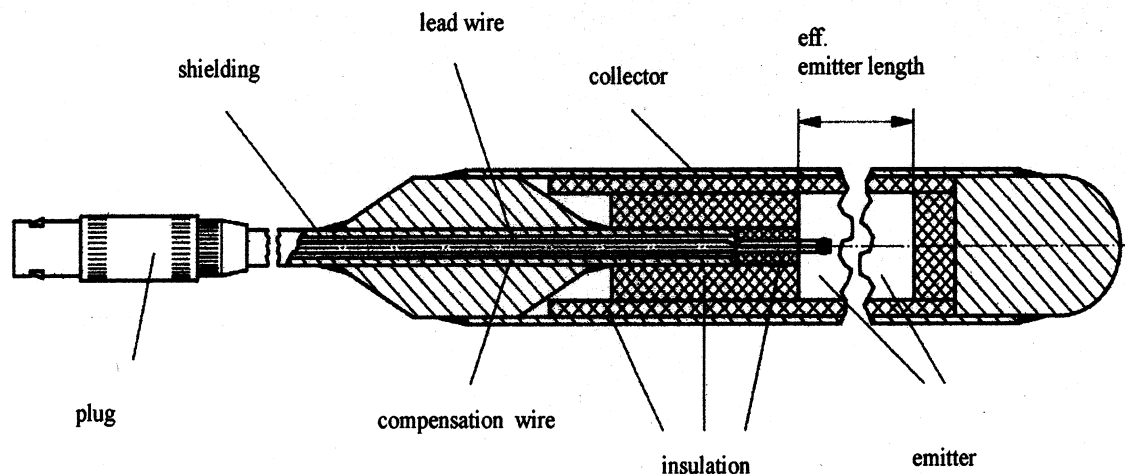


Fig. 3. Cross section of the rhodium emitter SPND applied for the reference measurement

The authors did not have the possibility to check the geometrical data of the detector (there was not any other detector to be taken apart). Nevertheless, the material compositions were compared with data found in literature. The densities of the emitter, insulation and collector were calculated using the mass and dimension data of [5] and compared to literature data from several sources (these were equivalent to 1%). The comparison yielded a significant discrepancy: the calculated densities proved to be 3% smaller, 5% greater and 21% smaller than the literature values for the emitter, insulation and collector, respectively.

Table I. Geometrical and material data of the SPND used for the reference measurement (from [5])

Materials	
Emitter	Rh
Insulation	MgO
Collector	Inconel-600
Cable shield	Inconel-600
Wire	Cu
Wire insulation	Al ₂ O ₃ por
Dimensions	
Radius of emitter	0,5 mm
Outer radius of insulator	0,85 mm
Outer radius of collector	1,1 mm
Cable length	10 m
Effective length of emitter	60 mm
Masses	
Emitter	0,5670 g
Insulation	0,366 g
Collector	0,62 g

Since Ref. [5] was not considered as a primary technical documentation of the detector, we decided to use literature data. The effect of discrepancies was studied by sensitivity analysis.

3.3. COMPUTATION OF THE NEUTRON FLUX DISTRIBUTION IN THE EMITTER

In order to determine the spatial neutron flux distribution in the emitter, the rhodium cylinder of 0.5 mm radius and 60 mm length was modelled for MCNP as ten cells of concentric cylindrical rings, each being 0.05 mm thick. The cylindrical rings were used as volumetric flux tallies with multipliers for tallying the reaction rate of the ¹⁰⁴Rh (n,γ) reaction.

Preliminary calculations have shown that the flux distribution along the axis of the detector was quite flat (variation is less than 1.3% in the 60 mm interval) due to the fact that the detector was located at the vertical symmetry plane of the reactor. Therefore, the 60 mm long cylindrical ring shaped cells were not divided vertically.

The neutron transport calculation was performed in criticality (*kcode*) mode. In view of the extremely small volume of the ten cylindrical tally cells a huge number of neutrons had to be started, corresponding to a very long CPU time.

The reaction rate was calculated in three neutron energy groups (thermal: 0 - 0.5 eV, intermediate: 0.5 eV – 821 keV and fast: 821 keV – 20 MeV). The shape of the spatial distribution of the reaction rate was of the expected character. The largest change in the reaction rate was observed in the intermediate group, where the rate at the centerline is only one-third of that obtained at the surface of the emitter. The depression in the thermal group was much smaller, the ratio of centerline to surface reaction rate being 0.77. The reaction rate in the fast group was practically constant along the radius (within the 1,7% average statistical uncertainty). The distribution of the neutron capture reaction with respect to the energy groups is as follows: the thermal neutrons are responsible for approximately 80% of all the reactions, while the remaining 20% is due to the intermediate neutrons. The neutron capture due to fast neutrons is negligible, i.e. more than 3 orders of magnitude less than that of the thermal neutrons.

Fig. 4 represents the total (i.e. summed for the 3 energy groups) reaction rate as a function of the distance from the axis of the detector. Since the number of reactions in each cell is obtained by multiplying this distribution with the volume of the given cylindrical ring, which is linearly increasing, it is obvious that major portion of the capture reactions occur close to the surface of the emitter.

3.4. CALCULATION OF THE TRANSPORT OF ELECTRONS AND PHOTONS IN THE DETECTOR REMOVED FROM THE REACTOR CORE

After determining the spatial distribution of the reaction rate of the neutron captures in the emitter, this distribution was taken equal to the distribution of the electrons emitted from the beta-decay of rhodium. As outlined earlier, the electron and photon transport calculation was performed using a much simpler model containing only the detector and its immediate vicinity. The actual contents of this model were the detector, the holder and a water cylinder of 11 cm diameter and 18 cm height.

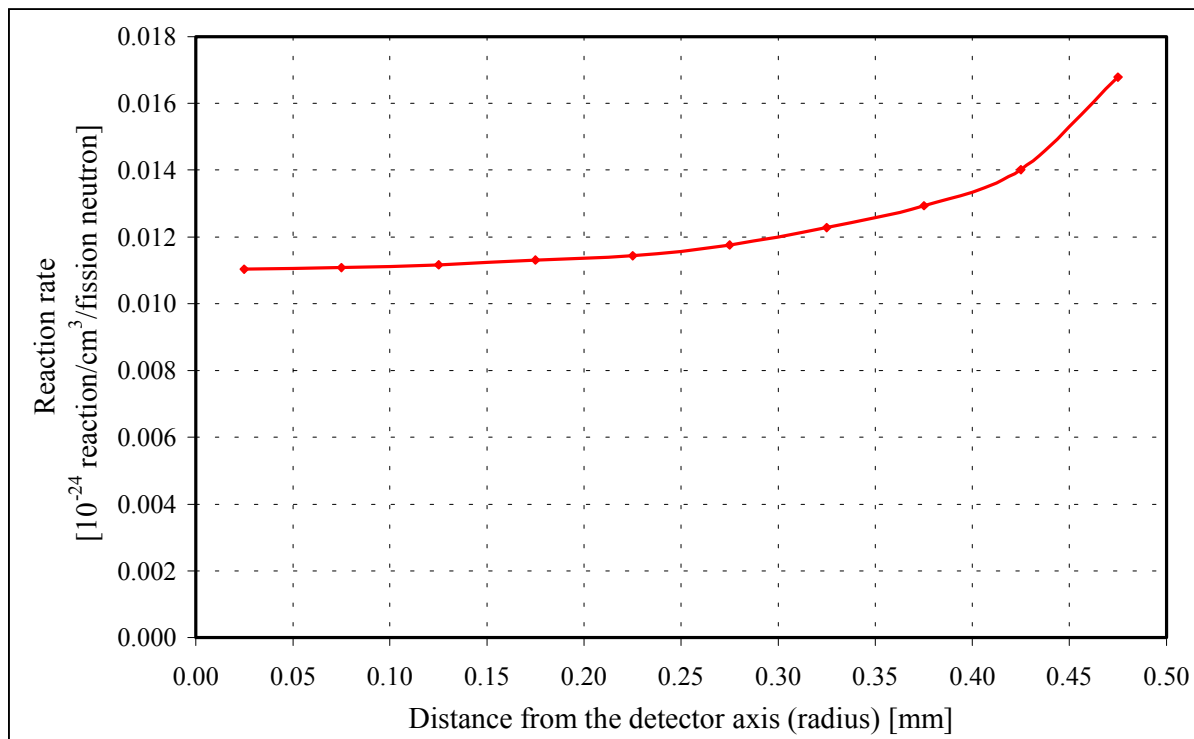


Figure 4. Neutron capture reaction density in the emitter

In order to investigate the electron and photon transport processes in an adequately detailed fashion, the emitter as well as the insulator and the collector were also divided into cylindrical rings of a uniform 0.05 mm thickness (the height was 60 mm). Thus the emitter was divided into ten (same as in the neutron model), while the insulator and collector into seven and five rings, respectively. This equidistant division was extended to a water cylinder of 0.4 mm surrounding the detector.

With the application of the above described spatial electron source distribution, MCNP was run in *mode e p*. By turning on the photon transport, it was ensured that not only the transport of primary electrons but also that of the secondary photons and photon induced electrons was taken into account.

The electron cutoff energy was the default 1 keV. In the following sections, the electrons followed by MCNP will be called „transport” electrons, while those getting below the cutoff energy will be called „stopped” (slowed down) electrons.

Surface current tallies were used to calculate the current of the „transport” electrons passing through each of the cylindrical surfaces moving in positive and negative directions with respect to the normal of the surfaces. The calculational results are shown graphically in Fig. 5. The differences of the currents were used to determine the spatial distribution of the charge deposition density of the “stopping” electrons in the insulator. The latter distribution was applied for the calculation of the electrostatic field evolving in the insulator using the INSPOT program. The result of the calculation of the spatial distribution of the charge deposition density is shown in Fig. 6. It is well visible that the charge deposition density is decreasing at a significant degree in the insulator layer, moving away from the emitter. Therefore, the widespread and widely used Warren model [7], which assumes constant charge deposition over the insulator, cannot be applied for calculations of high standard. With the aid of the INSPOT program it has been demonstrated that in the case of the rhodium emitter detector investigated the radius of the maximum potential is significantly (approximately 7%) smaller than the Warren critical radius. This change results in 9.5% detector current increase compared to the Warren approximation.

By correcting the “transport” electron currents with the currents due to the evolving electrostatic field of the electrons stopped in the insulator, the equilibrium detector current has become 13.1 nA.

4. SENSITIVITY STUDIES

A detailed sensitivity analysis on different detector characteristics (density of the emitter and insulator, diameter of the emitter, and thickness of the insulator), as well as on the *ESTEP* parameter used in the MCNP electron-transport calculation has been carried out in order to find the cause of the significant (more than 25%) discrepancy between the measured and calculated currents. It was found that the emitter density has the most significant influence on the calculated current. As a result of three different effects (change in the neutron flux depression, in the (n,g) reaction rate, and in the electron escape probability from the emitter) 10% decrease of the rhodium density causes 7% increase of the current. Since no direct information was available on the manufacturing technology of the emitter, it is possible that this material was made in a powder metallurgy procedure, and in this case the density might be 10 to 15% lower than the theoretical maximum applied in the calculations. This would decrease the discrepancy between the measured and calculated currents to 15-18%.

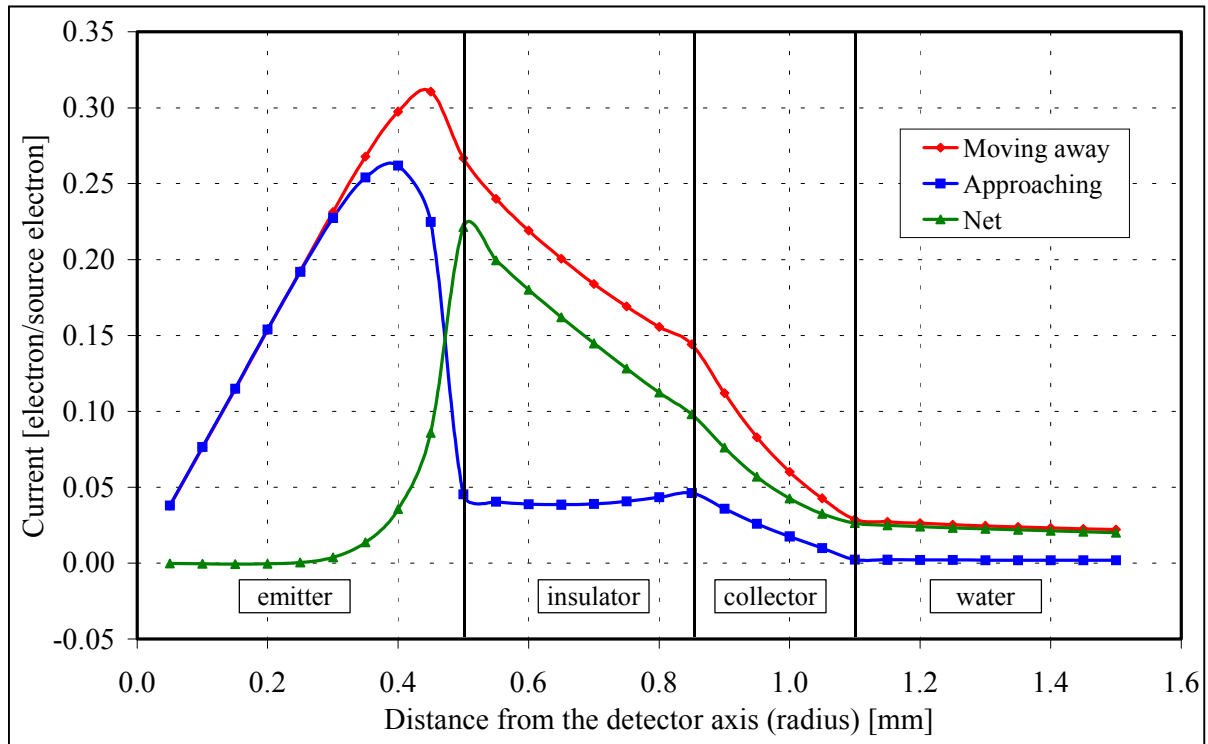


Figure 5. Currents of the “transport” electrons moving away from and approaching the detector axis, and the difference of the two currents vs. distance from the axis.

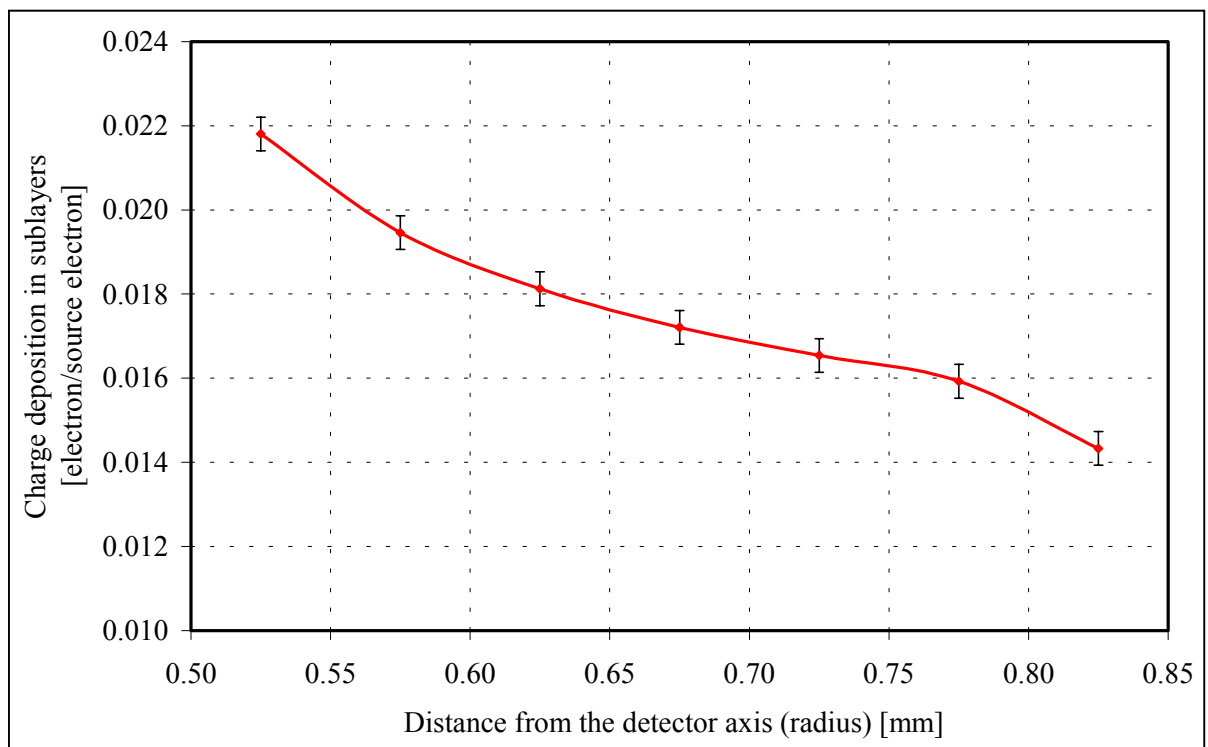


Figure 6. Charge deposition in the sublayers of the insulation as a function of the distance from the detector axis.

Another fact that may have a very strong influence on the value of the calculated current is the shape of the energy spectrum used to model beta-decay. In the Fermi-theory of the energy distribution of the electrons emitted from beta-decay there is an atomic number and energy dependent correction factor, which describes the Coulomb-interaction of the electrons and the nucleus. Concerning this correction factor the related literature is rather reticent and different publications give dissimilar curves [8,9]. Our calculations have shown that the neglect of the Fermi correction factor may introduce as large as 30% difference in the calculated current. Accordingly, our investigation regarding the shape of the beta-spectrum will be continued.

CONCLUSION

In spite of the fact that SPNDs are used widely in the NPP practice, the operational mechanism of these detectors, the ratio of the current components of different origin and the behaviour of the detector in transient situations are not known to a sufficient depth. The primary reason for it is that the neutron, photon and electron processes must simultaneously be followed when modelling the operation, at the same time taking into account the electrostatic field evolving in the insulator region. Our investigations have shown that the 4C version of MCNP, supplemented with a program calculating the electrostatic field, is capable of studying the processes taking place in SPNDs. Nevertheless, due to the uncertainty of some nuclear data and parameters (cross sections, half-lives, beta-spectrum etc.) an SPND calculational benchmark project would be of great expedience.

REFERENCES

- [1] I. Pázsit, "On the possible use of the neutron current in core monitoring and noise diagnostics", *Ann. Nucl. Energy*, Vol. **24**, No. 15, pp. 1257-1270 (1997)
- [2] P.Lindén, J.K. H. Karlsson, B. Dahl, I. Pázsit, G. Pór, "Localisation of a neutron source using measurements and calculation of the neutron flux and its gradient", *Nucl. Inst. Methods in Phys. Res. A*, Vol. **438**, pp. 345-355 (1999)
- [3] S. Avdic, P. Lindén, I. Pázsit, "Measurement of neutron current and its use for the localisation of a neutron source", *Nucl. Inst. Methods in Phys. Res. A*, Vol. **457**, pp. 607-616 (2001)
- [4] J.F. Briesmeister (ed.), "MCNP - A General Monte Carlo N-Particle Transport Code, Version 4C", LA-13709-M, UC700 (March 2000)
- [5] B. Hellmich, J. Fiedler, J. Runkel, D. Stegemann, G. Pór, D. Bódizs, "The Influence of Different SPN-Detector Materials to the Result of Neutron Noise Analysis", *Proceedings of the ANS International Conference on the Physics of Nuclear Science and Technology*, Long Island New York, 1998 October 5-8 (1998)
- [6] E. Browne, R.B. Firestone, W.S. Shirley (ed.), "Table of Radioactive Isotopes", John Wiley & Sons, New York (1986)
- [7] H.D. Warren, "Calculational Model for Self-Powered Neutron Detectors", *Nucl. Sci. Eng.*, Vol. **48**, pp. 331-342 (1972)
- [8] K.S. Krane, "Introductory Nuclear Physics", John Wiley & Sons, New York (1988)
- [9] K.N. Mukhin, "Experimental Nuclear Physics", Mir Publisher, Moscow (1987)